crystals

MDPI

Article

Synthesis and Characterization of (Ca,Sr)$[C_2O_4]\cdot nH_2O$ Solid Solutions: Variations of Phase Composition, Crystal Morphologies and in Ionic Substitutions

Aleksei V. Rusakov *, Mariya A. Kuzmina, Alina R. Izatulina and Olga V. Frank-Kamenetskaya *

Crystallography Dept., Institute of Earth Sciences, St. Petersburg State University, 7/9, University emb., 199034 St. Petersburg, Russia; m.kuzmina@spbu.ru (M.A.K.); alina.izatulina@spbu.ru (A.R.I.)

* Correspondence: alex.v.rusakov@gmail.com (A.V.R.); o.frank-kamenetskaia@spbu.ru (O.V.F.-K.); Tel.: +7-921-924-2229 (A.V.R.)

Received: 14 November 2019; Accepted: 6 December 2019; Published: 8 December 2019

Abstract: To study strontium (Sr) incorporation into calcium oxalates (weddellite and whewellite), calcium-strontium oxalate solid solutions (Ca,Sr)$[C_2O_4]\cdot nH_2O$ (n = 1, 2) are synthesized and studied by a complex of methods: powder X-ray diffraction (PXRD), scanning electron microscopy (SEM) and energy dispersive X-ray (EDX) spectroscopy. Two series of solid solutions, isomorphous (Ca,Sr)$[C_2O_4]\cdot(2.5 - x)H_2O$) (space group I4/m) and isodimorphous $Ca[C_2O_4]\cdot H_2O$(sp.gr. $P2_1/c$)–$Sr[C_2O_4]\cdot H_2O$(sp.gr. $P\bar{1}$), are experimentally detected. The morphogenetic regularities of their crystallization are revealed. The factors controlling this process are discussed.

Keywords: calcium oxalate; strontium oxalate; solid solutions; ionic substitutions; weddellite; whewellite; X-ray powder diffraction; scanning electron microscopy; EDX spectroscopy

1. Introduction

Natural calcium oxalates dihydrous weddellite $Ca[C_2O_4]\cdot(2.5 - x)H_2O$ and monohydrous whewellite $Ca[C_2O_4]\cdot H_2O$ are widespread biominerals. They often form in the human body, for instance, a major part of the stones in the human urinary system consist of both [1,2]. These minerals also are found in salivary stones and other human pathogenic formations [3–5]. Besides, weddellite and whewellite often occur in crustose and foliose lichen thalli on the surface of Ca-bearing rocks and minerals [6–9]. Oxalate crystallization is a result of the interaction between metabolites of lichens and associated microscopic fungi with an underlying stone substrate in this case [10–14].

The crystal structure of monoclinic whewellite (space group $P2_1/c$) and tetragonal weddellite (sp.gr I4/m) of renal stones are well known [15–21]. Variations of weddellite unit cell parameters are well explained by the variable water content [18–20]. There is no evidence of ionic substitutions occurring at calcium sites of calcium oxalate crystal structures of renal stones. The complex multicomponent composition of the crystallization medium (of urea and of other human physiological liquids), however, allows for the probability of such substitutions [22]. The probability of Cd–Ca substitutions in synthetic whewellite is proposed by McBride et al., 2017 [23].

We found strontium impurities in weddellite and whewellite crystals in lichen thalli on Sr-bearing apatite rock via energy-dispersive X-ray (EDX) spectroscopy [9]. It allows us to suggest that Sr^{2+} ions leach from fluorapatite and substitute Ca^{2+} ions in oxalates. Synthetic strontium oxalates, monohydrate and dihydrate, have been reported by Baran, Sterling and Christensen, Hazen [7,15,24]. The tetragonal $Sr[C_2O_4]\cdot(2.5 - x)H_2O$ is isotypic to weddellite and, similarly, contains a variable number of water molecules. The monohydrate, $Sr[C_2O_4]\cdot H_2O$, belongs to the triclinic crystal system (sp gr. $P\bar{1}$).

This suggests the presence of two series of solid solutions, isomorphous (Ca,Sr)$[C_2O_4]\cdot(2.5 - x)H_2O$ (sp.gr. I4/m) and isodimorphous $Ca[C_2O_4]\cdot H_2O$(sp.gr. $P2_1/c$)-$Sr[C_2O_4]\cdot H_2O$ (sp.gr. $P\bar{1}$).

To clarify the patterns of Sr^{2+} ion incorporation into calcium oxalates (whewellite and weddellite), we synthesize (Ca,Sr)$[C_2O_4]\cdot nH_2O$ (n = 1, 2) solid solutions and study the variations of their phase composition and crystal morphologies as well as in ion substitutions.

2. Materials and Methods

2.1. Synthesis

Ca–Sr oxalates were crystallized by precipitation from aqueous solutions (0.5 L volume) containing calcium chloride ($CaCl_2$, 99% purity, Vekton), strontium nitrate ($Sr(NO_3)_2$, 99% purity, Vekton), sodium oxalate (1.5 mmol, $Na_2C_2O_4$, 98% purity, Vekton) and citric acid (6.5 mmol, $C_6H_8O_7\cdot H_2O$, 99% purity, Vekton). The atomic ratios of Sr/(Sr + Ca) cations ranged from 0 to 100%. The total amount of Ca^{2+} and Sr^{2+} ions was 5 times higher than the content of oxalate ions in each synthesis.

A non-stoichiometric composition of the solution and the presence of citric acid were used to stabilize weddellite formation [25]. The pH range of the solutions was 4.6–6.1 due to the small additions of solutions of NaOH (NaOH, 99%, Vekton) or HCl (HCl, 35–38 wt.% aqueous solution, 99.9% purity, Vekton). The syntheses were carried out at room temperature (22–25 °C), with the exposure of the solution for five days until complete precipitation. The resulting precipitate was filtered off, washed with distilled water and dried in air at room temperature. The precipitate consisted of fine-grained white crystalline powder, each 0.5 L solution volume provided around 200 mg of it.

2.2. Methods

2.2.1. X-Ray Powder Diffraction (PXRD)

The method was used to determine the phase composition of the precipitates. The measurements were performed using a Bruker « D2 Phaser » powder diffractometer (CuKα radiation of wavelength λ = 1.54178 Å). X-ray diffraction patterns were collected at room temperature in the range of 2θ = 3–60° with a step of 0.02°. Phase identification was carried out using the ICDD PDF-2 Database (release 2016). The unit cell parameters and coherently scattering domain (CSD) size were refined by using TOPAS 4.2 software [26].

2.2.2. Scanning Electron Microscopy (SEM) and Energy-Dispersive X-Ray (EDX) Spectroscopy

Scanning electron microscopy and energy-dispersive X-ray spectroscopy were used for the identification of calcium oxalates and for estimating calcium and strontium content in their crystals. Tetragonal weddellite and monoclinic whewellite crystals and their intergrowths were identified on SEM images by their previously described morphological features [12,27].

The study was carried out by means of a Zeiss Supra 40MP electron microscope, equipped with a variable-pressure secondary electron (VPSE) detector and Hitachi S-3400N with energy dispersive attachment AzTec Energy 350, at an accelerating voltage of 2 or 5 kV (depending on the image resolution). Magnification range varied from 100x to 1000x. Two SE detectors (secondary electron Everhart–Thornley), as well as a BSE detector (scintillation detector based on the highly sensitive YAG crystal with the resolution of 0.1Z of the atomic number) were used. The specimens were applied on two sided conducting tape and were coated with carbon (~15 nm). EDX analysis was performed by a standardless method that is generally reliable for elements with Z > 10. The mineral standards used were diopside (Ca) and celestine (Sr).

3. Results

3.1. X-Ray Powder Diffraction

The results of PXRD (Table 1, Figure 1) showed that, in the absence of strontium in the solution, the obtained precipitate was represented almost exclusively by weddellite (Figure 1a).

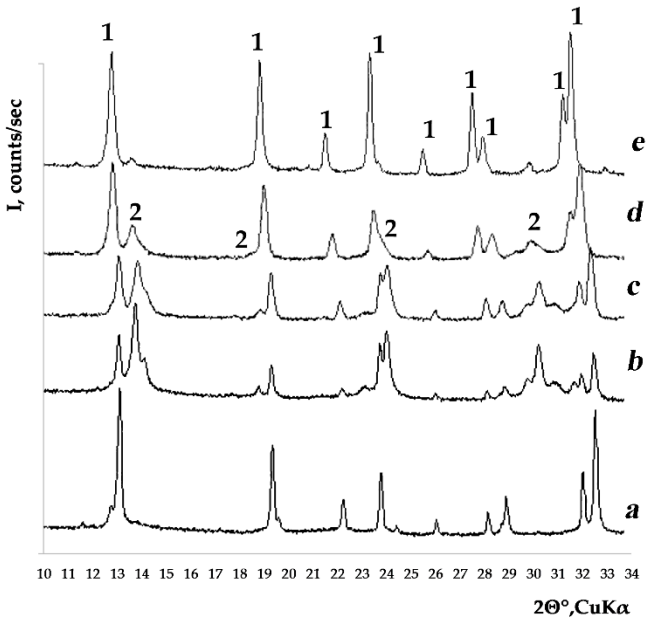

Figure 1. Typical XRD patterns of precipitates (1—weddellite, 2—whewellite), obtained from solutions with different atomic ratio Sr/(Sr + Ca), %: **a**—0; **b**—5; **c**—35; **d**—70; **e**—100.

Accompanying the addition of a small amount of strontium to the solution (Sr/(Sr + Ca) ≤ 30%), the precipitate became dominated by calcium oxalate monohydrate whewellite (Figure 1b). Weddellite content ranged from 23 to 34%. Concurrently, at Sr/(Sr + Ca) = 25–30%, traces of calcium oxalate trihydrate caoxite ($Ca[C_2O_4]\cdot 3H_2O$) were recorded in the precipitate (Table 1). Along with an increase of strontium content in the solution, the amount of whewellite in the precipitate decreased, while weddellite content increased, and at a ratio of Sr/(Ca + Sr) ~40%, these oxalates were present in the precipitate in almost equal amounts (Figure 1c). A further increase of strontium content in the solution (40% < Sr/(Sr + Ca) ≤ 80%) saw weddellite gradually start to prevail (Figure 1d). Accompanying a higher strontium content in the solution, the precipitate became close to monophasic—it is almost solely represented by weddellite (Figure 1e).

Along with the increase of strontium in the solution (and, consequently, in the formed crystals), the parameters of the weddellite tetragonal unit cell increased: ***a*** from 12.341 to 12.770 Å, ***c*** from 7.356 to 7.529 Å (Table 2). Linear parameters of monoclinic whewellite also increased: ***a*** from 6.289 to 6.396 Å, ***b*** from 14.576 to 14.860 Å, ***c*** from 10.120 to 10.367 Å (Table 2). The irregular fluctuations of the angle β value increased after Sr/(Sr + Ca) ≥ 40% (Table 2).

The average CSD size in Sr-containing weddellites varied from 162 to 71 nm and was smaller than 269 Å in Ca-weddellite. The minimum values of average CSD size (smaller than 100 Å) were observed at intermediate Sr/(Sr + Ca) ratios in solutions of 50–70%. Regarding Sr-containing whewellite, the average CSD sizes were from 57 to 28 Å, with an increase of strontium in the solution (Sr/(Sr + Ca) from 15 to 75), i.e., no less than two-times less than in weddellite (Table 2). Generally, the CSD size of the whewellite crystals gradually decreased with an increase in Sr content in the solution (up to the ratio Sr/(Sr + Ca) = 75%).

Table 1. Weddellite content in oxalate precipitate and strontium concentration in solution and in synthesized oxalates (via EDX).

Sample	Sr/(Ca + Sr) in Solution, %	Wd Content in Oxalate Precipitate, wt%	Sr Content in Crystal Phase, wt%		Sr/(Sr + Ca) in Crystal Phase, %	
			Wd	Wh	Wd	Wh
1	0.0	99.9	0.00	0.00	0.0	0.0
2	5.0	28.0	8.71	4.44	4.2	2.1
3	10.0	23.0	14.45	7.84	7.2	3.8
4	15.0	24.0	18.47	11.17	9.4	5.4
5	20.0	30.0	26.75	15.58	12.6	7.8
6	25.0	34.0 *	26.39	17.31	13.8	8.7
7	30.0	32.0 *	29.40	22.63	16.0	11.8
8	35.0	57.0	35.50	21.25	20.1	11.0
9	40.0	51.0	35.32	24.07	20.0	12.7
10	45.0	66.0	42.70	25.41	29.7	17.4
11	50.0	81.0	48.03	31.55	34.2	24.0
12	60.0	90.0	56.77	42.14	37.5	25.0
13	65.0	93.0	57.03	45.78	37.8	27.9
14	70.0	78.0	64.29	49.58	45.2	31.0
15	75.0	86.0	72.76	54.31	55.0	35.5
16	80.0	96.0	77.70	No data	61.4	No data
17	85.0	99.8	83.72	No data	70.2	No data
18	90.0	99.8	87.09	No data	75.5	No data
19	95.0	99.8	92.81	No data	85.5	No data
20	100.0	99.5	100.00	No data	100.0	No data

* Caoxite (2 wt%) is present in the precipitate.

Table 2. Oxalate unit cell parameters and average coherent scattered domain (CSD) size.

Sample	Sr/(Sr + Ca) in Crystal Phase, %		X-Ray Powder Diffraction Data							
			Weddellite (sp gr I4/m)			Whewellite (sp gr $P2_1/c$)				
	Wd	Wh	*a*, Å	*c*, Å	CSD, nm	*a*, Å	*b*, Å	*c*, Å	β, deg	CSD, nm
1	0.00	0.00	12.341(1)	7.356(1)	269(5)	Whewellite not detected				
2	4.2	2.1	12.3568(10)	7.3624(6)	121(3)	6.2889(6)	14.5762(14)	10.1200(12)	109.568(8)	43(1)
3	7.2	3.8	12.3772(14)	7.3708(8)	93(3)	6.2942(8)	14.5936(18)	10.1312(12)	109.533(6)	47(1)
4	9.4	5.4	12.3968(8)	7.3810(4)	162(5)	6.2999(5)	14.6134(12)	10.1415(10)	109.563(6)	47(1)
5	12.6	7.8	12.4027(9)	7.3873(5)	110(2)	6.3026(5)	14.6166(12)	10.1482(10)	109.544(6)	46(1)
6	13.8	8.7	12.4211(5)	7.3927(3)	155(4)	6.3072(4)	14.6313(1)	10.1615(10)	109.546(7)	43(1)
7	16.0	11.8	12.4360(7)	7.4009(3)	140(4)	6.3122(5)	14.6491(11)	10.1716(11)	109.527(1)	43(1)
8	20.1	11.0	12.4629(8)	7.4033(4)	103(3)	6.3122(7)	14.6538(15)	10.1761(15)	109.545(1)	37(1)
9	20.0	12.7	12.4784(7)	7.4090(3)	110(3)	6.3169(7)	14.6666(15)	10.1836(16)	109.535(1)	40(1)
10	29.7	17.4	12.5112(5)	7.4255(2)	107(1)	6.3362(8)	14.7075(17)	10.2130(2)	109.579(2)	35(1)
11	34.2	24.0	12.5301(5)	7.4303(3)	95(1)	6.344(2)	14.725(3)	10.243(4)	109.65(3)	32(1)
12	37.5	25.0	12.5571(9)	7.4382(4)	60(1)	6.333(4)	14.769(7)	10.258(9)	109.39(8)	37(3)
13	37.8	27.9	12.5902(7)	7.4529(3)	91(2)	6.339(3)	14.817(6)	10.229(9)	109.11(6)	57(7)
14	45.2	31.0	12.5907(8)	7.4583(4)	71(1)	6.351(2)	14.790(5)	10.301(6)	109.56(4)	28(1)
15	55.0	35.5	12.6315(6)	7.4762(3)	102(2)	6.396(3)	14.860(8)	10.367(6)	110.07(5)	30(2)
16	61.4	No data	12.6540(5)	7.4839(3)	106(2)					
17	70.2	No data	12.7070(15)	7.4979(9)	184(7)					
18	75.5	No data	12.7384(5)	7.5133(3)	136(3)	No data				
19	85.5	No data	12.7698(6)	7.5286(3)	127(3)					
20	100.0	No data	12.8247(4)	7.5377(2)	194(5)					

3.2. Scanning Electron Microscopy (SEM) and Energy-Dispersive X Ray (EDX) Spectroscopy

SEM data on the phase composition of the synthesized calcium oxalates support the XRD data (Table 1, Figure 2).

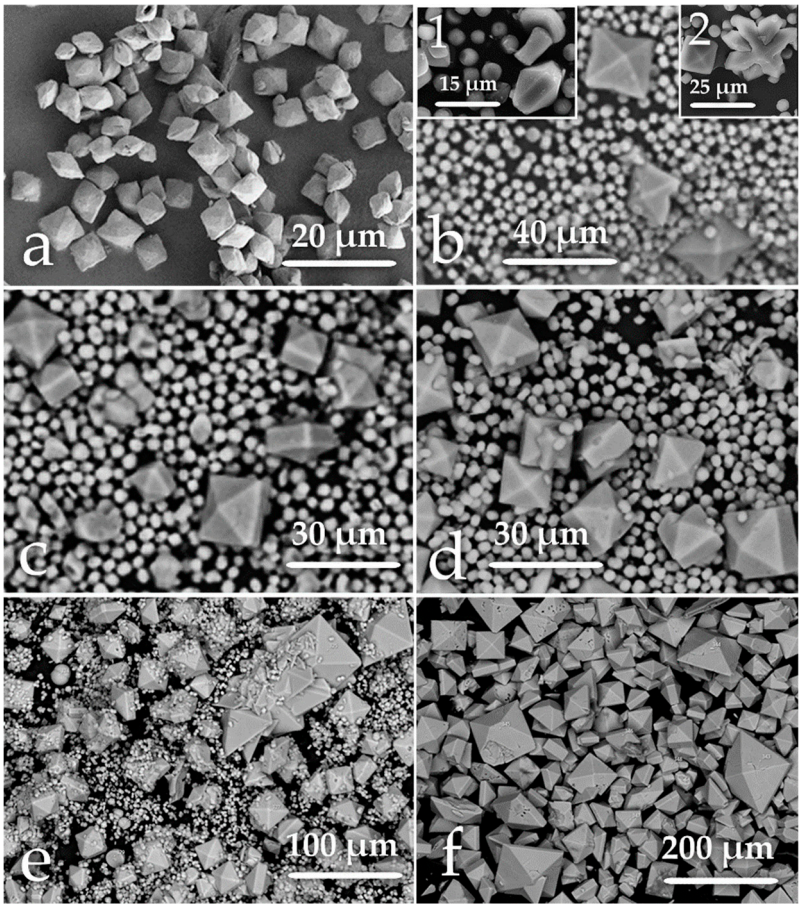

Figure 2. SEM images of formed (Ca,Sr)[C_2O_4]nH_2O (n = 1, 2) crystals, synthesized from solutions with different Sr/(Sr + Ca), % ratio: **a**: 0, **b**: 5, **c**: 20, **d**: 35, **e**: 70, **f**: 80.

SEM images clearly show that weddellite dipyramidal crystals represent calcium oxalates synthesized from strontium-free solutions, the dipyramidal base edge (**Dp**) of which does not exceed 5–6 microns (Figure 2a).

Found in the precipitate obtained from a solution with a ratio of Sr/(Sr + Ca) = 5%, small spherical spherulites of calcium oxalate monohydrate whewellite (diameter ~4–5 μm) prevail, among which there are individual weddellite crystals and their intergrowths (Figure 2b). According to EDX spectroscopy, strontium content in weddellite (Sr/(Sr + Ca) = 4.2%) is close to that in the solution and is two times greater than in whewellite (Sr/(Sr + Ca) = 2.1%). Weddellite crystals are defined by dipyramidal habit (**Dp** ~10–25 μm). Not very well-developed prism faces appear on smaller crystals (rib length between prism faces **Pr** = 3–4 μm, Figure 2b inset 1). The value of the average **Pr**/**Dp** ratio (which describes the degree of prism face development compared to dipyramid) is only 0.1. There also are twin intergrowths which form "quadruplets" consisting of two intergrown tetragonal dipyramids with a common fourth-order symmetry axis, with each dipyramid being rotated relative to each other around this axis of symmetry by 45° (Figure 2b inset 2).

Accompanying an increase in—ratio in the solution up to 30%, whewellite continues to prevail over weddellite (Figure 2c). According to EDX, Sr content increases in both phases (up to ratio Sr/(Sr + Ca) = 16.0% in weddellite and up to 11.8% in whewellite), but it decreases relative to the solution. The size of whewellite spherulites increases (average diameter ~6 μm, maximum 15 μm). Weddellite average crystal size also increases (**Dp** ~20–25 μm). While the number of weddellite crystals of dipyramidal-prismatic pattern increases, the prism face continues to develop: **Pr** ~10 μm, the **Pr**/**Dp** ~0.35.

When the Sr/(Sr + Ca) ratio in the solution reached 35–40%, the number of crystals of whewellite and weddellite became comparable (Figure 2d). According to EDX, Sr content continued to increase in both phases (up to Sr/(Sr + Ca) = 20% in weddellite and up to 11–13% in whewellite) and decreased relative to the solution. The size of whewellite spherulites was relatively small (5–6 microns in diameter, but reached 20 microns). Weddellite crystals also increased in size (**Dp** ~15–30 μm). All weddellite crystals had prism faces and the prism faces continued to develop (**Pr** ~10–20, **Pr**/**Dp** ratio ~0.40–0. 45).

When the ratio in the solution Sr/(Sr + Ca) ≤ 40%, weddellite began to prevail over whewellite. Two generations of weddellite crystals were observed in the precipitate: large dipyramidal (**Dp** up to 80 μm) and smaller dipyramidal-prismatic (**Dp** ~25 μm, **Pr** ~15–20 μm) (Figure 2e). The **Pr**/**Dp** ratio in weddellite crystals continued to increase and reached 0.56 at Sr/(Sr + Ca) = 50% in solution, and then began to decrease to 0.33 at Sr/(Sr + Ca) = 70%. The diameter of spherulites of whewellite decreased to 3–5 microns. According to EDX, the Sr/(Sr + Ca) ratio reached 55.0% in weddellite and 35.5% in whewellite.

Reaching a Sr/(Sr + Ca) ratio of 80% and more in the solution, weddellite crystallized almost solely, and was represented by large dipyramidal (200–250 μm) and smaller dipyramidal-prismatic (30–50 μm) crystals (Figure 2f). Attaining Sr/(Sr + Ca) = 85–95%, the development of the prism face slowed (**Pr** remained ~20 μm, the **Pr**/**Dp** ratio decreased to ~0.1). The Sr/(Sr + Ca) ratio in weddellite via EDX increased from 78 to 100%, approaching the value of this ratio in solution.

According to the EDX data, the Sr/(Sr + Ca) ratios of 29.7–45.2 in weddellite and of 17.4–31.0 in whewellite correspond to the minimum CSD size for both phases.

4. Discussion

The results of the study show that in all syntheses, solid solutions (Ca,Sr)$[C_2O_4]\cdot nH_2O$ (n = 1, 2) with a variable ratio of dihydrate and monohydrate phases are obtained. Phase and elemental composition of synthesized solid solutions, as well as the morphology of their crystals, is strongly relevant to strontium concentration in the solution.

4.1. The Effect of Strontium Concentration in Solution on Phase Composition of the Precipitate

The strontium content in the solution significantly affects the phase composition of the precipitate. Considering the absence of Sr^{2+} ions in the solution of non-stoichiometric composition (Ca/C_2O_4 = 5) containing citric acid, tetragonal calcium oxalate dihydrate weddellite (Figures 1a and 2a) is obtained, which is unstable in the crystallization field of monoclinic calcium oxalate monohydrate whewellite [17,21]. The addition of a small amount of Sr^{2+} ions (Sr/(Sr + Ca) = 5%) to this solution violates the conditions favorable for weddellite crystallization and leads to intensive crystallization of whewellite, the content of which in the precipitate exceeds the amount of weddellite by 2.6 times (Figures 1b and 2b, Table 1). Accompanying an increase in the strontium content in the solution, the amount of weddellite in the precipitate gradually increases and, at a ratio of Sr/(Sr + Ca) = 35–45%, matches the amount of whewellite (Figures 1c and 2d). A further increase in strontium content again creates conditions favorable for the crystallization of weddellite, the content of which in the precipitate begins to prevail (Figures 1d and 2e). Reaching an Sr/(Sr + Ca) ≥ 80% ratio in solution, the precipitate consists almost exclusively of weddellite. Thus, the presence of strontium in the crystallization medium can be favorable for the crystallization of both weddellite and whewellite, depending on the concentration.

4.2. Sr-Ca Ionic Substitutions in Solid Solutions

According to EDX, strontium is present in crystals of both calcium oxalate monohydrate and dihydrate (Table 1). The ratio Sr/(Sr + Ca) varies from 0 to 100% in weddellite and from 2.1 to 35.5% in whewellite. A narrower range of observed strontium concentrations in whewellite is explained by the synthesis conditions under which whewellite, unlike weddellite, precipitates only in solutions with an Sr/(Sr + Ca) ratio varying from 5 to 75% and always alongside weddellite. Altogether, strontium

content in weddellite is always higher than in whewellite by 1.4–2 times (Table 1), which indicates that the entry of Sr into whewellite is difficult compared to weddellite.

It is known that, despite the significant difference in ionic radii (r_{Ca}^{VIII} = 1.12 Å, r_{Sr}^{VIII} = 1.26 Å, [28]), Sr^{2+} ions easily replace Ca^{2+} ions which occupy large cavities coordinated by 7–9 cations in various crystal structures, like in apatite [29,30]. This suggests that all (or almost all) strontium recorded via EDX isomorphically substitutes calcium in its positions in weddellite and whewellite. A simultaneous increase of the unit cell parameters of weddellite and whewellite with the increasing Sr content (Figures 3 and 4) confirms this assumption.

An increase in the unit cell parameters of weddellite, primarily parameter *a*, also occurs with the increase of zeolite water (W_z) [18,19]. An increase of zeolite water amount in weddellite (from 0.13 to 0.37 apfu), however, leads to an increase in the *a* parameter by only 0.049 Å [18]. Conversely, the contribution of strontium to the increase of the weddellite parameter *a* is an order of magnitude greater; the change in parameter *a* reaches 0.469 Å (Figure 3a). The dependence of unit cell parameters of weddellite on strontium content is not linear and follows a second degree polynomial function (Figure 3). Violation of the linear correlation between the strontium content and the parameter values can be due, first, to the fact that when the Sr/(Sr + Ca) ratio reaches ~40% in weddellite (~60% in solution) Sr^{2+} ion entry into weddellite slows. Second, it is possible that at this strontium content, the amount of zeolite water in weddellite ceases to increase and a further slower increase in parameters occurs only due to an increase in strontium.

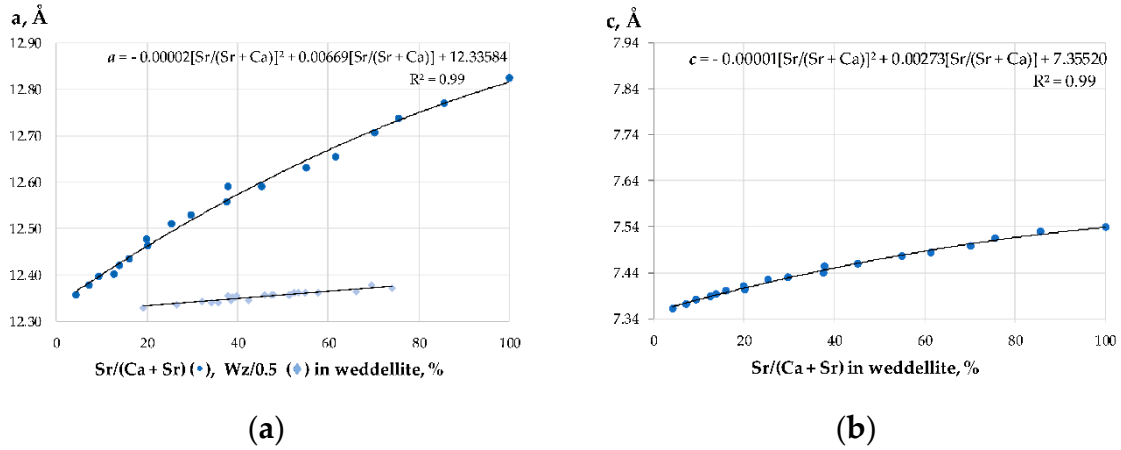

Figure 3. The increase of weddellite unit cell parameters: ***a*** unit cell parameter versus strontium (present study) and zeolite water [18] content, % (**a**); ***c*** unit cell parameter versus strontium content, % (**b**).

Seen at low strontium concentrations in whewellite (with Sr/(Sr + Ca) ratios in crystals varying from 2.1 to 12.7%; and in solution from 5 to 40%), there is a well-defined linear relationship between the values of linear parameters (***a***, ***b***, ***c***) and the content of strontium, while the angle β does not change significantly (Figure 4). The fluctuations of both linear parameters and angle β at higher strontium concentrations can be explained by desymmetrization (lowering the symmetry from monoclinic to triclinic), since the crystal structure of strontium oxalate monohydrate ($Sr[C_2O_4]\cdot H_2O$) is triclinic [7,24]. Desymmetrization may be associated with reciprocal turns of calcium polyhedra and oxalate groups, associated with the partial ordering of calcium and strontium atoms at the crystallographic sites. To the question of why desymmetrization is not at maximum in the middle of the series, further studies should be made.

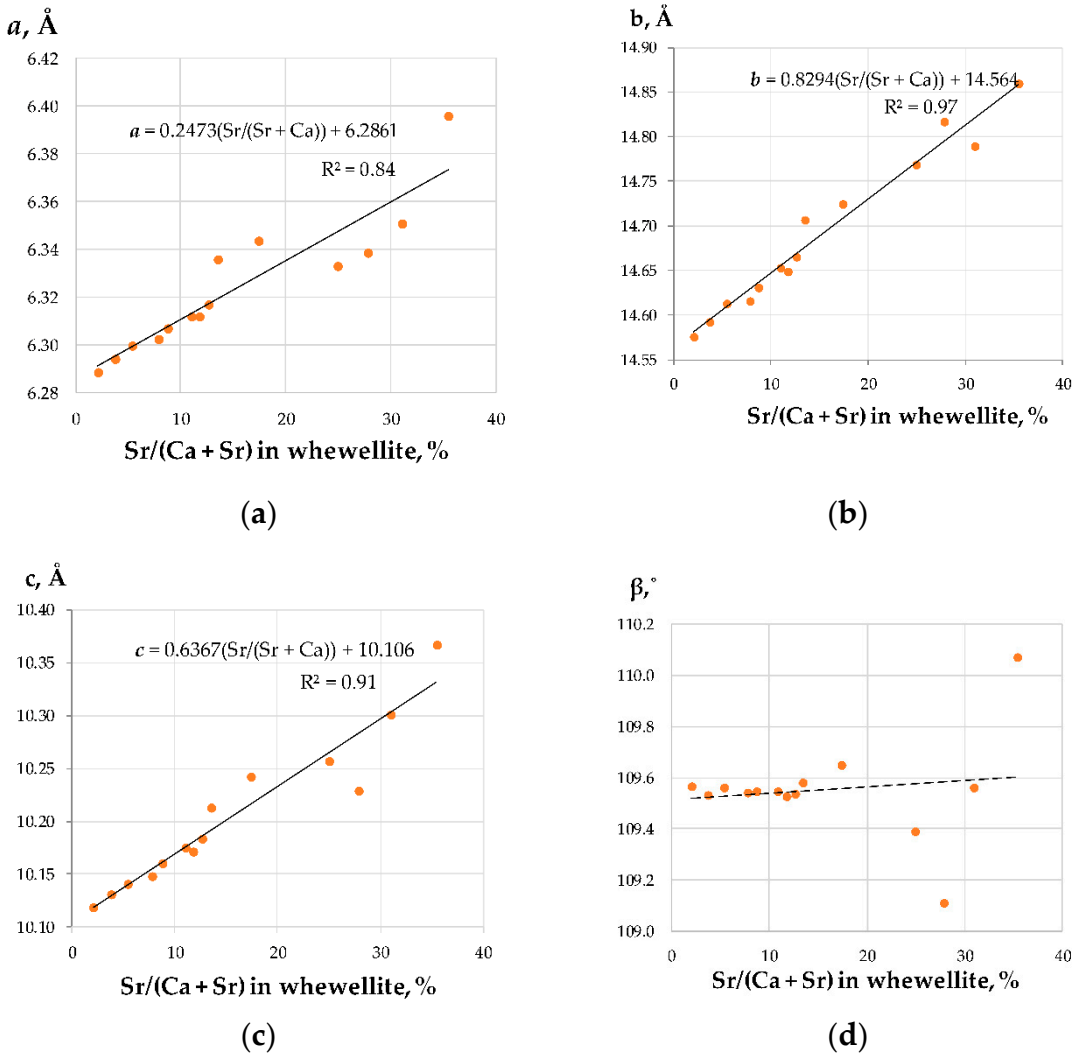

Figure 4. Variations of whewellite unit cell parameters versus strontium content, %: ***a*** (**a**); ***b*** (**b**); ***c*** (**c**); β (**d**).

Thus, assumption of the presence of two series of solid solutions, isomorphous (Ca,Sr)$[C_2O_4]\cdot(2.5 - x)H_2O$) (sp.gr. I4/m) and isodimorphous $Ca[C_2O_4]\cdot H_2O$(sp.gr. $P2_1/c$)–$Sr[C_2O_4]\cdot H_2O$(sp.gr. $P\bar{1}$), received experimental confirmation. A detailed study of the desymmetrization pattern of the monoclinic whewellite structure with strontium incorporation via single-crystal X-ray diffraction analysis is now in progress.

4.3. Morphogenetic Patterns of the Formation of Solid Solutions (Ca,Sr)$[C_2O_4]\cdot nH_2O$ (n = 1, 2)

4.3.1. The Effect of Sr Concentration in Solutions on Crystal Morphology

Regarding all variations of strontium content in solution (0 ≤ Sr/(Sr + Ca) ≤ 100%), weddellite is represented by dipyramidal and/or dipyramidal-prismatic crystals, and whewellite by round spherulites (Figure 2).

As strontium content in the solution increases, the size of the weddellite dipyramidal crystals grows as well: **Dp** varies from ~5–6 μm in pure calcium crystals to 30 μm at Sr/(Sr + Ca) = 35% (Figure 2a–d). Accompanying a further increase of strontium concentration in the crystallization medium, the formation of two weddellite crystal generations is clearly observed. Larger ones are mainly of dipyramidal pattern and smaller ones of dipyramidal-prismatic configuration (Figure 2e). The size of larger weddellite crystals increases with the increase of strontium concentration in the solution, from **Dp** = 30 μm at Sr/(Sr + Ca) = 35% to **Dp** = 200 μm at Sr/(Sr + Ca) = 80–95% (Figure 2f).

The size of smaller weddellite crystals also increases with the increase of strontium content, from **Dp** = 15 μm at Sr/(Sr + Ca) = 35% in solution to **Dp** = 50–60 μm at Sr/(Sr + Ca) = 80–95% in solution. Tetragonal prism faces of smaller weddellite crystals are well developed and the size of these faces along the prism edge also gradually increase with the increase of strontium content in the solution, from **Pr** = 3–4 μm at Sr/(Sr + Ca) = 5% (Figure 2b) to **Pr** = 20 μm at Sr/(Sr + Ca) = 70–80% (Figure 2e,f). The aspect ratio between the prism and dipyramid faces with the increase of strontium content in the solution increases from 0.1 (at Sr/(Sr + Ca) = 5%) to 0.56 (at Sr/(Sr + Ca) = 50%) and then it starts to decrease to 0.1 (at Sr/(Sr + Ca) = 95%).

Shown above, the first and last syntheses of the studied series (purely calcium and purely strontium solutions) are characterized by the formation of weddellite crystals in the form of a tetragonal dipyramid, which indicates optimal conditions for the precipitation of calcium and strontium oxalate dihydrate. The middle members in the weddellite series exhibit tetragonal prism faces in their pattern. The ratio between linear sizes of the prism and dipyramidal faces increases with the increase in strontium content in solution from 0.1 (at Sr/(Sr + Ca) = 5%) to 0.56 (at Sr/(Sr + Ca) = 50%), and then decreases to 0.1 (at Sr/(Sr + Ca) = 95%). Accordingly, with an increase in strontium in the crystallization medium from 5 to 50%, the initial prism growth rate increases significantly and then (at a ratio Sr/(Sr + Ca) ≥ 65%) begins to decrease. The slowdown in the growth rate of weddellite prism faces in the middle of the calcium-strontium series is most likely due to the deviation of the crystallization conditions from optimal.

Kuzmina et al [25] demonstrates that the crystallization of whewellite in the form of spherulites is common for solutions containing citrate ions and indicates a more rapid growth of whewellite (compared with weddellite) under the conditions of a higher supersaturation of the solution. The average diameter of whewellite spherulites is dependent on the content of Sr^{2+} cations in the solution. It first increases from 4 μm (at Sr/(Sr + Ca) = 5%, Figure 2b) to 6 μm (at Sr/(Sr + Ca) = 35–50%, Figure 2d), then it decreases to 1–2 μm (at Sr/(Sr + Ca) = 70–80%, Figure 2e,f) amid the decrease in the total amount of whewellite.

4.3.2. Sr-distribution in Oxalate System «Solution–Crystal»

The strontium concentration in oxalate monohydrate and oxalate dihydrate ($0 \leq Sr/(Ca + Sr) \leq 100\%$) depends on strontium concentration in the solution following a third degree polynomial function (Figure 5):

$$Sr/(Sr + Ca)_{Solution} = 0.0006[Sr/(Sr + Ca)_{wh}]^3 - 0.0815[Sr/(Sr + Ca)_{wh}]^2 + 4.3286[Sr/(Sr + Ca)_{wh}] - 5.4929,$$

$$Sr/(Sr + Ca)_{Solution} = 0.0001[Sr/(Sr + Ca)_{Wd}]^3 - 0.0266[Sr/(Sr + Ca)_{Wd}]^2 + 2{,}67[Sr/(Sr + Ca)_{Wd}] - 7.1757.$$

Fitting with a third degree polynomial function is necessary due to the fact that the difference between strontium content in the crystallization medium and in synthesized solid solutions increases in the middle of the corresponding series.

The described distribution of strontium in the oxalate "crystal-solution" system indicates that the incorporation of strontium ions into calcium oxalates from solutions with close to equal amounts of Ca and Sr is difficult, which can explain the decrease of weddellite prism face growth rate and the lowering of CSD sizes for both weddellite and whewellite.

The difference in strontium content between the solution and whewellite is greater than between the solution and weddellite (Figure 5), which supports a proposal for a more difficult incorporation of Sr^{2+} cations into whewellite than into weddellite. This effect can most likely be explained by the specific features of weddellite and whewellite crystal structures. This result also agrees well with the above conclusion that whewellite crystals grow more rapidly than weddellite crystals.

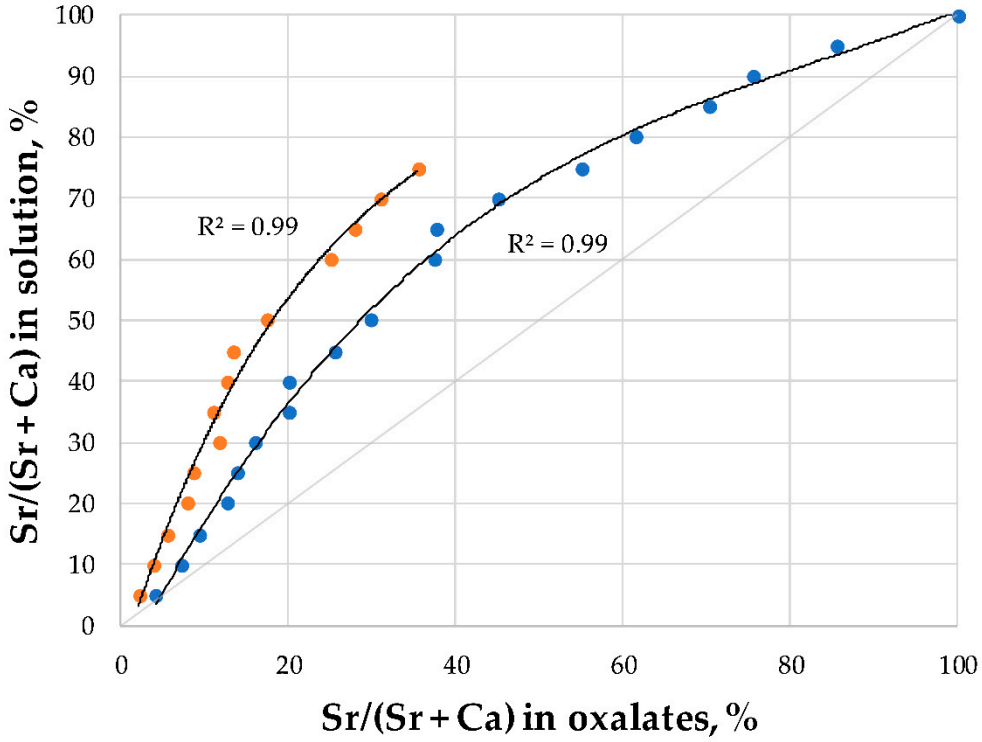

Figure 5. Sr/(Ca + Sr) ratio in the solution versus Sr/(Ca + Sr) ratio in the weddellite (●) and whewellite (●).

5. Conclusions

To clarify the patterns of Sr incorporation into calcium oxalates (whewellite and weddellite) the (Ca,Sr)$[C_2O_4]\cdot nH_2O$ (n = 1, 2) solid solutions were synthesized and studied by complex methods (PXRD, SEM and EDX). It was shown that phase and elemental composition of synthesized solid solutions, as well as the morphology of their crystals, is strongly relevant to Sr concentration in the solution. The presence of two series of solid solutions, isomorphous (Ca,Sr)$[C_2O_4]\cdot(2.5 - x)H_2O$) (sp.gr. I4/m) and isodimorphous $Ca[C_2O_4]\cdot H_2O$(sp.gr. $P2_1/c$)–$Sr[C_2O_4]\cdot H_2O$(sp.gr. $P\bar{1}$) was experimentally proven for the first time. The causes of a difficult incorporation of strontium ions into calcium oxalates (especially into whewellite) were discussed. Morphogenetic regularities of their formation were revealed.

The results of this work show the possibility of diverse ionic substitutions occurring at calcium sites of calcium oxalate crystal structures, which opens a new page in the crystal chemistry of oxalic acid salts. Among the oxalates found in nature, biofilm biominerals formed as a result of the interaction of metabolism products of lithobiotic community with bedrock are highly favorable to exhibit ionic substitutions at a global scale. The regularities of these ionic substitutions are determined by both the mineral and elemental composition of the underlying rock and the species composition of the microorganisms inhabiting them. The applied value of the obtained patterns lies in the field of the development of biotechnologies which use the oxalate microbial crystallization as a source of bioremediation for environments contaminated with toxic elements.

Author Contributions: Conceptualization (A.V.R. and O.V.F.-K.); Investigation (A.V.R., M.A.K. and A.R.I.); Methodology (A.V.R., O.V.F.-K. and M.A.K.); Visualization (A.V.R. and A.R.I.); Writing—original draft (A.V.R., M.A.K. and A.R.I.); Writing—review & editing (A.V.R. and O.V.F.-K.).

Funding: This research was funded by the Russian Science Foundation (grant 19-17-00141 to A.V.R., O.V.F.-K., M.A.K., A.R.I.).

Acknowledgments: The laboratory researches were carried out in Research Resource Centers of Saint Petersburg State University: XRD measurements—in the X-ray Diffraction Centre; SEM investigations—in the Interdisciplinary Resource Center for Nanotechnology and Centre for Geo-Environmental Research and Modelling (Geomodel).

Conflicts of Interest: The authors declare no conflict of interest.

References

1. Balaji, K.C.; Menon, M. Mechanism of stone formation. *Urolithiasis* **1997**, *24*, 1–11. [CrossRef]
2. Grases, F.; Costa-Bauza, A.; Garcia-Ferragut, L. Biopathological crystallization: A general view about the mechanisms of renal stone formation. *Adv. Colloid Interface Sci.* **1998**, *74*, 169–194. [CrossRef]
3. Kraaij, S.; Brand, H.S.; van der Meij, E.H.; de Visscher, J.G. Biochemical composition of salivary stones in relation to stone and patient-related factors. *Med. Oral Patol. Oral Cir. Bucal* **2018**, *23*, e540–e544. [CrossRef] [PubMed]
4. Nishizawa, Y.; Higuchi, C.; Nakaoka, T.; Omori, H.; Ogawa, T.; Sakura, H.; Nitta, K. Compositional Analysis of Coronary Artery Calcification in Dialysis Patients in vivo by Dual-Energy Computed Tomography Angiography. *Ther. Apher. Dial.* **2018**, *22*, 365–370. [CrossRef] [PubMed]
5. Kuranov, G.; Nikolaev, A.; Frank-Kamenetskaya, O.; Gulyaev, N.; Volina, O. Physicochemical characterization of human cardiovascular deposits. *J. Biol. Inorg. Chem.* **2019**, *24*, 1047–1055. [CrossRef]
6. Rusakov, A.V.; Frank-Kamenetskaya, O.V.; Zelenskaya, M.S.; Vlasov, D.Y.; Gimelbrant, D.E.; Knauf, I.V.; Plotkina, Y.V. Calcium oxalates in bio-films on surface of the chersonesus archaeological limestone monuments (Crimea). *Zap. Rmo (Proc. Russ. Mineral. Soc. Russ.)* **2010**, *5*, 96–104.
7. Baran, E.J. Review: Natural oxalates and their analogous synthetic complexes. *J. Coord. Chem.* **2014**, *67*, 3734–3768. [CrossRef]
8. Marques, J.; Gonçalves, J.; Oliveira, C.; Favero-Longo, S.E.; Paz-Bermúdez, G.; Almeida, R.; Prieto, B. On the dual nature of lichen-induced rock surface weathering in contrasting micro-environments. *Ecology* **2016**, *97*, 2844–2857. [CrossRef]
9. Frank-Kamenetskaya, O.V.; Ivanyuk, G.Y.; Zelenskaya, M.S.; Izatulina, A.R.; Kalashnikov, A.O.; Vlasov, D.J.; Polyanskaya, E.I. Calcium Oxalates in Lichens on Surface of Apatite-Nepheline Ore (Kola Peninsula, Russia). *Minerals* **2019**, *9*, 656. [CrossRef]
10. Ríos de los, A.; Cámara, B.; Cura del, M.Á.G.; Rico, V.J.; Galván, V.; Ascaso, C. Deteriorating effects of lichen and microbial colonization of carbonate building rocks in the Romanesque churches of Segovia (Spain). *Sci. Total Environ.* **2009**, *407*, 1123–1134. [CrossRef]
11. Sayer, J.A.; Gadd, J.M. Solubilization and transformation of insoluble inorganic metal compounds to insoluble metal oxalates by *Aspergillus niger*. *Mycol. Res.* **1997**, *6*, 653–661. [CrossRef]
12. Sturm, E.V.; Frank-Kamenetskaya, O.V.; Vlasov, D.Y.; Zelenskaya, M.S.; Sazanova, K.V.; Rusakov, A.V.; Kniep, R. Crystallization of calcium oxalate hydrates by interaction of calcite marble with fungus *Aspergillus niger*. *Am. Mineral.* **2015**, *100*, 2559–2565. [CrossRef]
13. Rusakov, A.V.; Vlasov, A.D.; Zelenskaya, M.S.; Frank-Kamenetskaya, O.V.; Vlasov, D.Y. The Crystallization of Calcium Oxalate Hydrates Formed by Interaction Between Microorganisms and Minerals. In *Biogenic—Abiogenic Interactions in Natural and Anthropogenic Systems*; Frank-Kamenetskaya, O., Panova, E., Vlasov, D., Eds.; Lecture Notes in Earth System Sciences; Springer: Cham, Switzerland, 2016; pp. 357–377. [CrossRef]
14. Zelenskaya, M.S.; Rusakov, A.V.; Frank-Kamenetskaya, O.V.; Vlasov, D.Y.; Izatulina, A.R.; Kuz'mina, M.A. Crystallization of Calcium Oxalate Hydrates by Interaction of Apatites and Fossilized Tooth Tissue with Fungus *Aspergillus niger*. In *Processes and Phenomena on the Boundary Between Biogenic and Abiogenic Nature*; Frank-Kamenetskaya, O., Vlasov, D., Panova, E., Lessovaia, S., Eds.; Lecture Notes in Earth System Sciences; Springer: Cham, Switzerland, 2020; pp. 581–603. [CrossRef]
15. Sterling, C. Crystal-structure of Tetragonal Strontium Oxalate. *Nature* **1965**, *205*, 588–589. [CrossRef]
16. Tazzoli, V.; Domeneghetti, C. The crystal structures of whewellite and weddellite: Reexamination and comparison. *Am. Mineral.* **1980**, *65*, 327–334.
17. Izatulina, A.R.; Yelnikov, V.Y. Structure, chemistry and crystallization conditions of calcium oxalates—the main components of kidney stones. In *Minerals as Advanced Materials I*; Krivovichev, S.V., Ed.; Springer: Berlin/Heidelberg, Germany, 2008; pp. 231–241.
18. Izatulina, A.R.; Gurzhiy, V.V.; Frank-Kamenetskaya, O.V. Weddellite from renal stones: Structure refinement and dependence of crystal chemical features on H_2O content. *Am. Mineral.* **2014**, *99*, 2–7. [CrossRef]

19. Rusakov, A.V.; Frank-Kamenetskaya, O.V.; Gurzhiy, V.V.; Zelenskaya, M.S.; Izatulina, A.R.; Sazanova, K.V. Refinement of the crystal structures of biomimetic weddellites produced by microscopic fungus *Aspergillus niger*. *Crystallogr. Rep.* **2014**, *59*, 362. [CrossRef]
20. Mills, S.J.; Christy, A.G. The Great Barrier Reef Expedition 1928–29: The crystal structure and occurrence of weddellite, ideally $CaC_2O_4{\cdot}2.5H_2O$, from the Low Isles, Queensland. *Mineral. Mag.* **2016**, *80*, 399–406. [CrossRef]
21. Izatulina, A.R.; Gurzhiy, V.V.; Krzhizhanovskaya, M.G.; Kuz'mina, M.A.; Leoni, M.; Frank-Kamenetskaya, O.V. Hydrated Calcium Oxalates: Crystal Structures, Thermal Stability and Phase Evolution. *Cryst. Growth Des.* **2018**, *18*, 5465–5478. [CrossRef]
22. Frank-Kamenetskaya, O.V.; Izatulina, A.R.; Kuz'mina, M.A. Ionic substitutions, non-stoichiometry, and formation conditions of oxalate and phosphate minerals of the human body. In *Biogenic—Abiogenic Interactions in Natural and Anthropogenic Systems*; Frank-Kamenetskaya, O., Panova, E., Vlasov, D., Eds.; Lecture Notes in Earth System Sciences; Springer: Cham, Switzerland, 2016; pp. 425–442. [CrossRef]
23. McBride, M.B.; Frenchmeyer, M.; Kelch, S.E.; Aristilde, L. Solubility, structure, and morphology in the co-precipitation of cadmium and zinc with calcium-oxalate. *J. Colloid Interface Sci.* **2017**, *486*, 309–315. [CrossRef]
24. Christensen, N.; Hazell, R.G. Thermal analisys and crystal structure of tetragonal strontium oxalate dihydrate and of triclinic strontium oxalate hydrate. *Acta Chem. Scand.* **1998**, *52*, 508. [CrossRef]
25. Kuz'mina, M.A.; Rusakov, A.V.; Frank-Kamenetskaya, O.V.; Vlasov, D.Y. The influence of inorganic and organic components of biofilms with microscopic fungi on the phase composition and morphology of crystallizing calcium oxalates. *Crystallogr. Rep.* **2019**, *64*, 161. [CrossRef]
26. Bruker, A.X.S. Topas V4.2: General Profile and Structure Analysis Software for Powder Diffraction Data. Available online: http://www.topas-academic.net/ (accessed on 6 December 2019).
27. Zuzuk, F.V. *Urinary Calculus Mineralogy*, *2*; Volynsk State University: Luzk, Ukraine, 2003; p. 507. (In Ukranian)
28. Shannon, R.D. Revised effective ionic radii and systematic studies of interatomic distances in halides and chalcogenides. *Acta Crystallogr.* **1976**, *32*, 751–767. [CrossRef]
29. Heijligers, H.J.M.; Driessens, F.C.M.; Verbeeck, R.M.H. Lattice parameters and cation distribution of solid solutions of calcium and strontium hydroxyapatite. *Calcif. Tissue Int.* **1979**, *29*, 127–131. [CrossRef] [PubMed]
30. Nikolaev, A.; Kuz'mina, M.; Frank-Kamenetskaya, O.; Zorina, M. Influence of carbonate ion in the crystallization medium on the formation and chemical composition of CaHA–SrHA solid solutions. *J. Mol. Struct.* **2015**, *1089*, 73–80. [CrossRef]